How to combine direct and indirect adiabatic cooling into an air handling unit for resilient tertiary buildings

Antoine Breteau, Emmanuel Bozonnet, Patrick Salagnac, Jean-Marie Caous

BUILDING SIMULATION 2025 24–27 AUG BRISBANE CARBON AND CLIMATE RESPONSIVE

International Building Performance Simulation Association

How to combine direct and indirect adiabatic cooling into an air handling unit for resilient tertiary buildings

Antoine Breteau[1,2], Emmanuel Bozonnet[1], Patrick Salagnac[1], Jean-Marie Caous[2]
[1]LaSIE (UMR CNRS 7356), La Rochelle Université, Av. M. Crépeau, 17042 La Rochelle, France
[2]BLUETEK, ZI Nord les Pins, 37230 Luynes, France

Abstract

In this article we propose various indicators to highlight the performances and the resilience of an air-handling unit (AHU) that can integrate both direct and indirect adiabatic cooling. This combined adiabatic strategy enhances the cooling performance during heatwaves. We developed the control strategy of the integrated system into a TRNSYS numerical model. Considering continental, Mediterranean, arid subtropical and equatorial climates, we analyzed best operation strategies for a typical office building. The multicriteria approach highlights the lower efficiency under equatorial climates. The system performs better in arid environments, in this case study the Mediterranean climate is better regarding the water consumption while the subtropical arid climate is better regarding the fan consumption.

Key Innovations

- Development of a model for an AHU with two adiabatic cooling modules coupled to a tertiary building.
- Evaluation of system performance through specific indicators.

Practical Implications

This paper presents a TRNSYS numerical model coupling an air handling unit to a typical tertiary building. It is utilized to assess the performance of the AHU equipped with two adiabatic modules, using specific indicators. The results obtained offer several practical applications:

- *Control optimization*: enhancement of system control strategies to increase efficiency under different operating conditions.
- *Advanced design approach*: adaptation of the system according to building type and the external climate, informed by new specific indicators.
- *Overall performance improvement*: improved energy efficiency and greater potential for system application in different contexts.

These results contribute to improved integration and management of adiabatic systems within the building sector.

1. Introduction

The year 2024 could be the hottest on record, with global average temperatures projected to be 1,54°C above pre-industrial levels (WMO, 2024). The 6th IPCC report stresses that human activities, in particular the increasing use of air conditioning, are contributing to this temperature rise. Although effective in hot weather, air conditioning also exacerbates global warming (IPCC, 2022). Faced with this challenge, alternative solutions such as passive adiabatic cooling are being developed to reduce indoor building temperatures while limiting energy consumption and minimizing environmental impact (PROFEEL, 2021).

According to the Annex 80 of the IEA EBC (Attia et al., 2022), adiabatic cooling is a promising solution for resilient cooling. These systems reduce indoor temperatures by evaporating water as warm air passes through a moist, porous material (Watt, 1997). Direct systems introduce fresh, moist air, while indirect systems use a heat exchanger to prevent the introduction of moisture (Xuan et al., 2012). Systems that combine these two approaches dynamically optimize performance, although they are more complex and are often integrated with air handling unit (PROFEEL, 2021).

This article focuses on this indirect adiabatic cooling strategy, combined to free cooling and direct adiabatic cooling in order to maximize the performance of the AHU. Compared the direct adiabatic system only, we avoid thermal discomfort and building disorders due to moisture and high ambient humidity. The generic principle of an indirect adiabatic cooling system consists to circulate a secondary airflow that is directly cooled and humidified by water evaporation, while the supplied airflow to the building is indirectly cooled by an heat exchanger (Kowalski and Kwiecień, 2020; Mohammed et al., 2022).

There are several existing typologies of standalone indirect systems, such as those using the Maisotsenko cycle (M-cycle) (Maisotsenko et al., 2003), the dew point systems (Jia et al., 2019), and the regenerative systems (Kashyap et al., 2020).

There are also adiabatic cooling systems that are coupled to the air handling units (AHUs). In our case study, the indirect adiabatic cooling unit is integrated within the air extraction duct (secondary airflow) that indirectly cools the supplied airflow within the heat exchanger. These systems are mostly used in tertiary buildings.

In the following, we first define the performance indicators to assess the multiple aspects of adiabatic cooling. This study focuses on AHU and adiabatic cooling for tertiary buildings. The behavior of the system is analyzed for

https://doi.org/10.26868/25222708.2025.1364

four different climates, highlighting the prevalence of free cooling or adiabatic modes of operation. The performance results differ in terms of resilience, thermal comfort, and energy or water consumption.

2. Case study

2.1 System integration into the building

The study area is an office of an existing building. It is located at the second floor of a three-story concrete building (Figure 1) – floor area 82 m^2, and 3,10 m height.

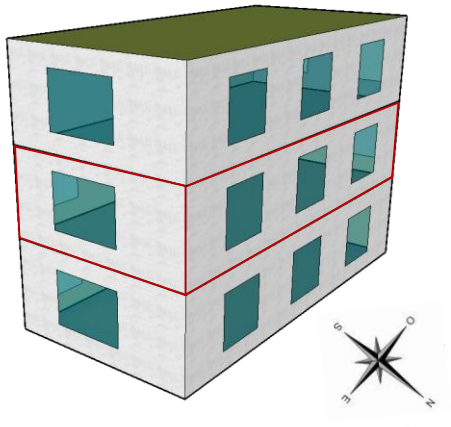

Figure 1: Building

Exterior walls are insulated with 12 cm rock wool on the inside. This office space has 7 occupants from 8 a.m. to 6 p.m., from Monday to Friday, except for the periods from August 10 to 31 and December 19 to 31. Each occupant uses a laptop and monitor for office-type activities. The lighting is provided by 27 W lamps. The air permeability is 1 m^3/(h/m^2) at 4 Pa. The minimum airflow is 175 m^3/h (25 m^3/h per occupant), while the max AHU airflow for free cooling is 650 m^3/h (2,5 ACH) (Figure 3). This flow represents the optimum balance between adequate overheating reduction and moderate supply air flow (Figure 2).

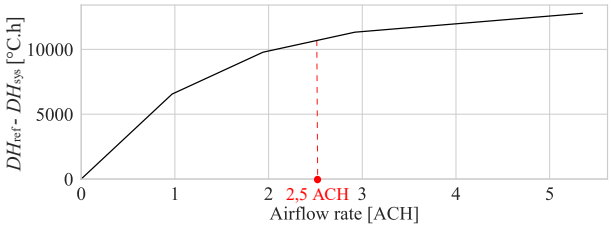

Figure 2: System sizing

In order to determine the optimum supply airflow rate, we studied the evolution of the reduction of the indoor overheating by the system (*DH* – equation (4)) as a function of the system air change rate. Figure 2 shows that the reduction reaches a horizontal asymptote. So we chose at 2,5 ACH as a reasonable value regarding the cooling evolution.

The AHU integrates two adiabatic modules (Figure 3): indirect (IEC) on the return air (AR), and direct (DEC) on the supply air (AS).

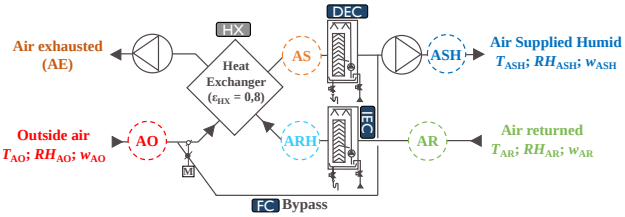

Figure 3: Air handling unit diagram

The heat exchanger mode HX (ε_{HX} = 0,8) and two fans (0,21 W/(m^3/h)) allows to operate in:

- indirect mode IEC (HX enabled),
- combined indirect/direct mode IEC/DEC (HX enabled),
- free cooling mode FC (bypass of heat exchanger HX),
- Heat exchanger mode HX

The system principle is explained in Figure 4.

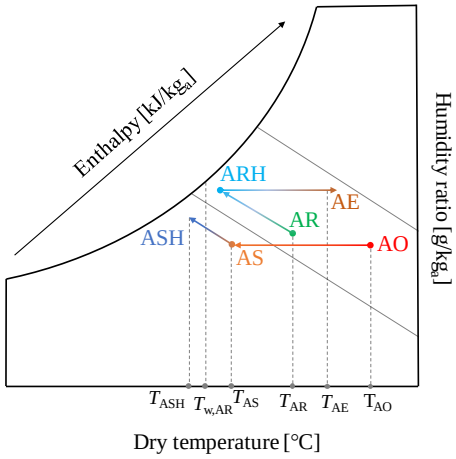

Figure 4: Psychrometric diagram

In indirect mode, an indirect adiabatic system (IEC) first cools and humidifies the extracted air from the building (AR). This cooled air then passes through a heat exchanger (HX) where it cools the fresh air before being supplied to the building (AS). During this process, the warm outside air (AO) heats the exhaust air (AE) in return, as it passes through the heat exchanger. When the indoor temperature becomes too high, the direct adiabatic system (DEC) is activated. The air leaving the heat exchanger (AS) is then cooled and humidified a second time by this system, resulting in even cooler, more humid air (ASH) before being blown into the building. In contrast, when HX operates alone, the fresh air exchanges calories with the return air of building without adding humidity before being blown into the building (AS). Free cooling mode cools the building directly with outside air (AO).

The integration of adiabatic systems (Figure 5) increases the cooling capacity of the AHU, allowing it to achieve a supply air temperature low enough to meet the thermal constraints of the space

https://doi.org/10.26868/25222708.2025.1364

Figure 5: Adiabatic cooling system

The system studied (Figure 5) incorporate Munters Celdek® 5090 cellulose evaporative media (ε_{sat} = 0,85), a circulation pump (40 W), a water tank, a water distributor (without spray) and a regulation module.

The control system adjusts operating modes according to set temperatures, which vary according to building occupancy (Figure 6).

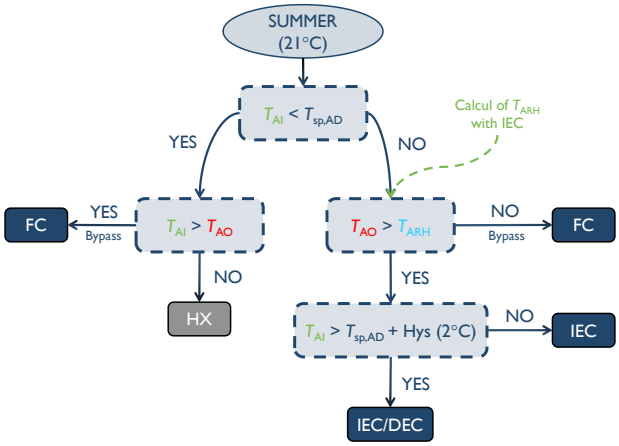

Figure 6: System regulation

Its operation is based on ON/OFF control, which is only activated in summer when the indoor temperature exceeds 21°C. Various conditions, detailed in the flowchart in Figure 6, then determine the operating mode according to the indoor and outdoor temperatures. The system operates in free-cooling mode FC when the indoor temperature T_{AI} is lower than the indirect adiabatic setpoint $T_{sp,\,AD}$ and the outdoor air temperature T_{AO} is lower than the indoor temperature. Otherwise, it switches to conventional double-flow heat exchanger mode HX. Then, indirect adiabatic mode IEC is activated when two conditions are met:

- IEC adiabatic mode setpoint temperature $T_{sp,AD}$ is reached, set at 24°C in this study.
- The cooling potential of the IEC module is sufficient to cool the building.

To verify this second condition, an intermediate calculation of the T_{ARH} temperature is performed. This theoretical calculation is used to determine if activating the IEC system would provide a real cooling benefit to the building. If this is not the case, free-cooling takes over. The direct system (DEC) is activated when the indoor temperature exceeds the adiabatic set point by 2°C (Hys).

2.2 Methodology and numerical model

The numerical model of the AHU has been developed using the TRNSYS© building dynamics simulation software. This model is essentially based on the saturation efficiency of the adiabatic systems (1)(2) and the mixing law of the HX (3).

$$\epsilon_{sat,IEC} = \frac{T_{AR} - T_{ARH}}{T_{AR} - T_{wb,AR}} \quad (1)$$

$$\epsilon_{sat,DEC} = \frac{T_{AS} - T_{ASH}}{T_{AS} - T_{wb,AS}} \quad (2)$$

$$\varepsilon_{HX} = \frac{h_{AO} - h_{AS}}{h_{AO} - h_{ARH}} \quad (3)$$

T, T_{wb}, and h represent the dry bulb temperature, wet bulb temperature, and enthalpy of the air, respectively. These were measured at different points in the system (Figure 4). The saturation efficiency of adiabatic systems depends on the air inlet conditions. The efficiency of HX is based on the enthalpy differences between the exchanger inlets and outlets.

To analyze the climate resilience of the system and highlight variations in performance, we selected four contrasting climates that represent very different profiles. The Mediterranean climate, represented by Carpentras (France), is characterized by hot, dry summers and mild winters. The continental climate, represented by Paris (France), offers relatively hot summers and moderate winters. The arid subtropical climate, typical of Abu Dhabi (United Arab Emirates), remains hot and dry throughout the year. Finally, the equatorial climate, as found in Singapore, is characterized by constant temperatures between 22°C and 32°C, high relative humidity of 70-80 %, and cool nights. Simulations were performed over a medium-term heat wave period (2040-2060), considering an adverse emissions scenario. They were generated according to the method described in Annex 80 (Attia et al., 2022), using CORDEX data (Machard et al., 2020).

Several indicators of comfort, performance and resilience are studied. Indoor comfort is assessed using the T_{op} (operative temperature) and *SET** indicators. *SET** represents the dry temperature of an isothermal environment at 50 % relative humidity, where occupants experience the same thermal and thermoregulatory constraints as in the real environment (Gagge et al., 1986).

Cumulative thermal discomfort can be assessed using the total number of degree-hours exceeding a temperature threshold $T_{i,lim}$, providing a normalized measure of overheating as a function of T_{op}. For each equivalent temperature indicator, whether T_{op} or *SET**, the discomfort limit

https://doi.org/10.26868/25222708.2025.1364

can be defined based on current regulations or corresponding neutral discomfort thresholds. This makes it possible to calculate discomfort degree hours (*DH* or *SETH*) according to equation (4).

$$DH \text{ or } SETH = \sum_{h=1}^{n} \left(T_i - T_{i,lim}\right)_{T_i > T_{i,lim}} \quad (4)$$

The limit temperature $T_{i,lim}$ is determined using the *PMV* method defined by ASHRAE 55 (ASHRAE, 2013), assuming *PMV* = 0, an air velocity of 0,2 m/s, a metabolism of 1,4 met and a cover of 0,5 clo. According to the ASHRAE psychrometric comfort diagram, a T_{op} temperature of 26°C corresponds to a *SET** of 25,6°C.

The resilience of the system was evaluated through the α indicator, which measures the resistance of the building to climate change and the risk of overheating, based on the ratio between the *IOD* and *AWD* indicators (Hamdy et al., 2017). The *IOD* is an average overheating temperature which is the sum of the positive values of the difference between the operating temperature (T_{op}) of the zone and the limit comfort temperature of the same zone (26°C), averaged over the sum of the total number of occupied hours. *AWD* is used to quantify the severity of outdoor thermal conditions. It's the positive sum of the difference between the outdoor air temperature T_{AO} and the base temperature T_b (26°C) reduced to the number of hours of occupation.

$$\alpha = \frac{IOD}{AWD} \quad (5)$$

If $\alpha < 1$ then the building is able to eliminate external thermal stress in the long term and if $\alpha > 1$ then the building is unable to eliminate external thermal stress in the long term.

To assess the performance of the system, we first analysed the maximum average daily *SET** temperature at occupancy achieved by the system ($SET^*_{dailymax}$). Then, we evaluated this performance by comparing the reduction in indoor overheating by the system ($\Delta SETH$) with the volume of water evaporated V_w by adiabatic cooling systems (6) and the energy consumption of fans C_{fan} (7).

$$\frac{\Delta SETH}{V_w} = \frac{SETH_{ref} - SETH_{sys}}{V_w} \quad (6)$$

$$\frac{\Delta SETH}{C_{fan}} = \frac{SETH_{ref} - SETH_{sys}}{C_{fan}} \quad (7)$$

Finally, the performance was analyzed by the coefficient of performance (*COP*), which is the ratio between the amount of energy useful for cooling C_{AC} and the amount of energy consumed by the system $C_{consumed}$.

$$COP = \frac{C_{AC}}{C_{consumed}} \quad (8)$$

3. Results and discussions

3.1 System operation

First, the system operation was analyzed. Figure 7 shows the operating times for the different AHU operating modes.

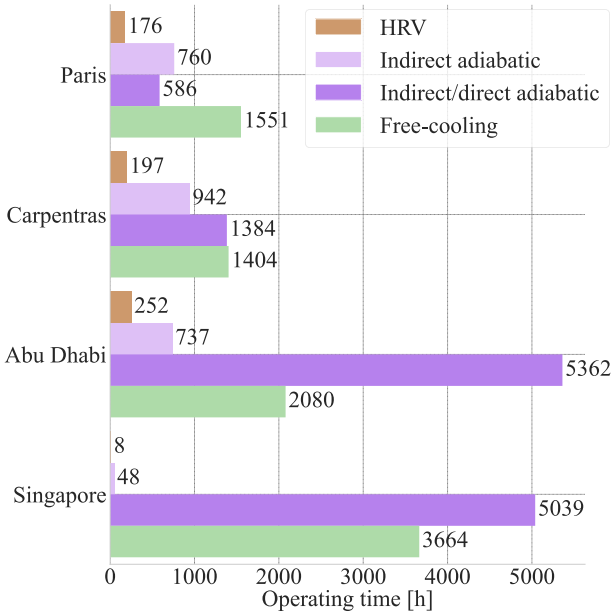

Figure 7: Operating time of the different AHU modes

Figure 7 illustrates the differences between air conditioning operation in different climates. In hot climates, such as Abu Dhabi (5 362 h) and Singapore (5 039 h), the indirect/direct mode dominates due to the high outdoor heat and therefore constant cooling demand. In Singapore, free-cooling is also important, with 3 664 h, i.e. 43 % more than in Abu Dhabi, while the heat exchanger mode is almost non-existent (8 h). In temperate climates, such as Paris and Carpentras, the modes are more balanced: free-cooling predominates in Paris (1 551 h), while indirect/direct mode is more common in Carpentras (1 384 h vs. 586 h in Paris). These results show that in hot climates, indirect mode alone is not sufficient and direct mode is required, while free cooling is particularly well suited to temperate and humid climates. The HX mode is rarely used, whatever the climate, underlining the importance of adapting air handling units to the climatic conditions.

Figure 8 shows the significant differences observed between different climates in terms of fan energy consumption.

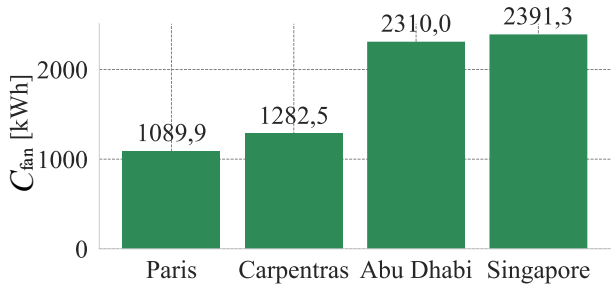

https://doi.org/10.26868/25222708.2025.1364

Figure 8: Fan energy consumption

This graph shows that the energy consumption of fans varies little from one climate to another. In Carpentras, it is only 17 % higher than in Paris. These results are directly related to the behavior of the system, which is used more in Carpentras, especially in indirect/direct mode. For more extreme climates, the consumption in Singapore is 3 % higher than in Abu Dhabi, due to the more intensive use of free cooling in Singapore than in Abu Dhabi.

Figure 9 shows the amount of water evaporated by adiabatic systems.

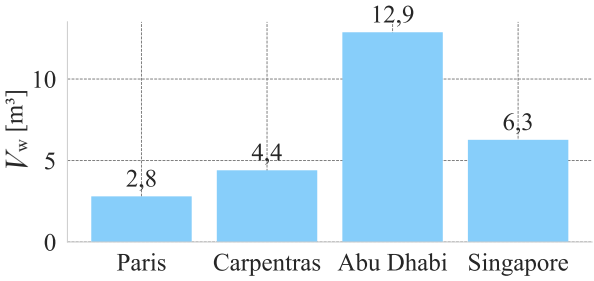

Figure 9: Evaporated water volume

This graph shows a large fluctuation in the consumption of evaporated water. In Abu Dhabi (hot subtropical climate), the system evaporated 12,9 m^3 of water, twice as much as in Singapore (equatorial climate) and more than four times as much as in Paris (temperate climate). This difference can be explained by the intensive use of adiabatic systems in hot, dry climates, where evaporation is more efficient than in humid climates such as Singapore. A similar trend can be observed for the Paris and Carpentras climates.

3.2 System performance

The performance of the system was analyzed by studying its effect on the overheating of the interior of building, in particular by evaluating its effect on the indoor degree-hours, calculated as a function of T_{op} (*DH*), but also of *SET** (*SETH*), to take into account the humid aspect of the air. Figure 10 shows the values of this overheating (*SETH* and *DH*) for all climates with and without system (reference).

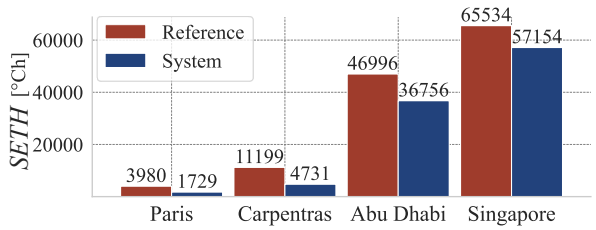

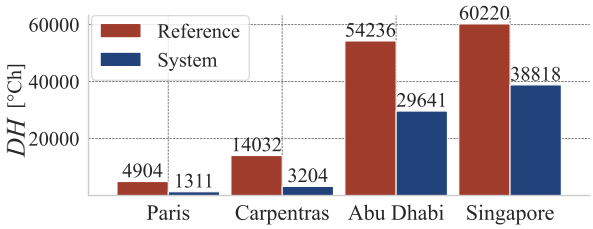

Figure 10: Indoor overheating (SETH and DH)

The graph shows similar trends for the *DH* and *SETH* indicators across climates. For the reference case, continental climates have the lowest discomfort and equatorial climates the highest. Discomfort is higher in extreme climates (Abu Dhabi, Singapore) than in temperate climates, and the impact of the system varies by climate. In hot, dry climates, the indirect/direct mode is used more often, which introduces more humid air and has a greater impact on comfort. With *DH*, the system reduces discomfort by 73 % in Paris and 77 % in Carpentras. Even though the system operates almost continuously, overheating (*DH*) remains high in climate of singapore. This is due to the high humidity, which limits the adiabatic cooling system efficiency because the air cannot cool sufficiently. On the other hand, when the relative humidity (*SETH*) is taken into account, the results show a smaller reduction in discomfort, especially in Singapore (13 % with *SETH* vs. 35 % with *DH*). This difference is explained by two factors:

- High outdoor humidity in equatorial climates limits the effectiveness of system, particularly in *SET** based thermal comfort analysis.
- Increased use of indirect/direct mode in these conditions introduces more humid air indoors, compared with indirect mode alone.

This difference is less pronounced in temperate climates, where *SETH* is down 56 % in Paris and 57 % in Carpentras.

The system performance was then evaluated using the coefficient of performance, as shown in Figure 11. This analysis was performed for three different configurations. The *COP* was calculated by simulating an air conditioning system AC that would replace the AHU. First, the *COP* of the AHU were calculated with all modules activated (9) and without the adiabatic modules (noAD) (10).

$$COP = \frac{C_{\mathrm{AC}}}{C_{\mathrm{fan}} + C_{\mathrm{pump}}} \quad (9)$$

$$COP_{\mathrm{noAD}} = \frac{C_{\mathrm{AC,noAD}}}{C_{\mathrm{fan,noAD}}} \quad (10)$$

The contribution of the adiabatic module in the AHU was then determined using equation (11):

https://doi.org/10.26868/25222708.2025.1364

$$COP_{AD} = \frac{C_{AC} - C_{AC,noAD}}{(C_{fan} - C_{fan,noAD}) + C_{pump}} \quad (11)$$

The amount of useful energy C_{AC} refers to the energy required by the air conditioning system to maintain the set-point temperature, which is defined as the indoor temperature obtained from simulations with the AHU.

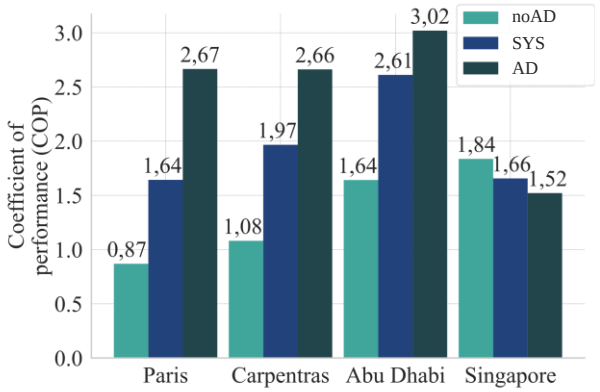

Figure 11: System performance coefficients with and without adiabatic systems

This graph illustrates the performance of the AHU in different climates, with and without adiabatic systems. Without adiabatic systems (noAD), the AHU in Singapore achieves a *COP* of 1,84, 12 % better than in Abu Dhabi. In Carpentras, the system absorbs more energy than it distributes (1,08). Overall, the addition of adiabatic systems (SYS) increases the performance of the AHU by 88 % for Paris and 82 % for Carpentras, except in the equatorial climate where the humidity of the climate reduces the *COP* by 10 % (from 1,84 to 1,66). Abu Dhabi offers the best performance with a *COP* of 2,61, 32 % higher than Carpentras. The *COP* of adiabatic systems alone (AD) reaches 3,02 in Abu Dhabi, two times higher than that recorded in Singapore. For French climates, the performance is almost identical. The addition of adiabatic systems, especially when they combine indirect and direct technologies, offers better performance in arid subtropical climates, while they are less efficient in very humid climates such as Singapore.

Finally, system performance was evaluated using specific performance and resilience indicators. Table 1 shows the absolute values of the obtained results. Results *without* the system are displayed in parentheses.

Table 1 : Absolute values of system performance in different climates

	Carpentras	Paris	Abu Dhabi	Singapore
$SET^*_{dailymax}$ [°C]	32,9 (*35,6*)	31,1 (*33,1*)	43,0 (*44,6*)	41,0 (*41,8*)
$\Delta SETH/C_{fan}$ [°C.h/kWh]	5,04	2,06	4,43	3,50
$\Delta SETH/V_w$ [°C.h/L]	1,47	0,80	0,79	1,33
α [-]	0,31 (*1,38*)	0,37 (*1,38*)	0,71 (*1,30*)	1,53 (*2,38*)

The results highlight the differences in the performance of the system according to the climates studied. Firstly, we find that the system reduces $SET^*_{dailymax}$ in all climates. However, under high humidity conditions, the impact of the system on the maximum values is less pronounced, as shown by the results for Singapore, where the reduction is only 0,8°C. This is mainly due to the intensive use of indirect and direct modes for a relatively small treated volume. Secondly, the impact of the system on the resilience of the building varies according to the climate. In most climates, the system helps to improve the resilience of buildings, particularly in Carpentras, where the coefficient α is reduced by 77 % (from 1,38 to 0,31). The impact of the system is similar in other French climates, although it is less pronounced in extreme climates such as Abu Dhabi, where the reduction is only 45 %. In equatorial climate (Singapore), however, the system does not allow the building to eliminate external thermal in the long term ($\alpha > 1$) .

Dry climates such as Carpentras and Abu Dhabi offer the best performance. Considering the reduction in overheating ($\Delta SETH$) in relation to the energy consumption of the fan, the system provides a gain of 5,04 °C.h/kWh and 4,43 °C.h/kWh, respectively. However, in more humid climates such as Paris, this performance is 59 % lower than in Carpentras (2,98 °C.h/kWh). The gain is more significant in arid climates, mainly due to a higher cooling potential, enhanced by outdoor conditions favorable to water evaporation. This enables the system to reduce the need for free-cooling and to limit the use of full fan power. Conversely, in humid climates, free-cooling is used to a greater extent, but the efficiency of adiabatic cooling is reduced by higher outdoor humidity.

The overheating reduction relative to the volume of water evaporated is better in Mediterranean climates, reaching 1,47 °C.h/L, 83 % better than Paris. In this climate, cooling potential is particularly high thanks to ideal outdoor conditions. Free-cooling is used as much as indirect/direct

https://doi.org/10.26868/25222708.2025.1364

mode, effectively limiting indoor overheating, particularly at night, while avoiding excessive water consumption. Equatorial climates, such as Singapore, show a gain of 1,33 °Ch/L, just 10 % less than Carpentras. This difference can be explained by more intensive use of free-cooling, which considerably reduces indoor overheating (3664 hours). Indirect/direct mode is also widely used, but with relatively low water evaporation (6,3 m^3) in relation to operating time. This system limits overheating while minimizing water consumption.

We then evaluated the performance of the system using relative values (reference without system 0 %), which we grouped into a radar chart (Figure 12). The 100 % relative performance values were specifically defined for the dimensionless indicators $(\Delta SETH/V_W)_{ad}$ (12) and $(\Delta SETH/C_{fan})_{ad}$ (13), based on the best performances obtained from simulations conducted across more than 10 different climates.

Thus, we determined that:

- The maximum $\Delta SETH/V_W$ was reached in Carpentras, with a value of 1,47 °C.h/L.
- The maximum $\Delta SETH/C_{fan}$ was observed in Carpentras, with a value of 5,04 °C.h/kWh.

These indicators are respectively defined by the *perceived cooling cumulative per liter consumed* and *perceived cooling cumulative per kWh consumed*. They are defined by the following expressions:

$$\left(\frac{\Delta SETH}{V_w}\right)_{ad} = \frac{1}{\left(\frac{\Delta SETH}{V_w}\right)_{max}} \left(\frac{\Delta SETH}{V_w}\right) \quad (12)$$

$$\left(\frac{\Delta SETH}{C_{fan}}\right)_{ad} = \frac{1}{\left(\frac{\Delta SETH}{C_{fan}}\right)_{max}} \left(\frac{\Delta SETH}{C_{fan}}\right) \quad (13)$$

For the other indicators, the maximum values were defined consistently with these references, considering 100 % performance, which corresponds to a situation where DH = 0 °C.h.

Cumulative cooling corresponds to the relative reduction in DH between the situation with the system and the reference situation (without the system). It is expressed by the ratio (14):

$$1 - \frac{DH_{sys}}{DH_{ref}} \quad (14)$$

This ratio measures the improvement made by the system in terms of DH reduction.

Similarly, we can assess the effect of the system on thermal comfort by considering the *cumulative cooling sensation* with $SETH$ (15).

$$1 - \frac{SETH_{sys}}{SETH_{ref}} \quad (15)$$

The dimensionless value of *overheating escalation factor* corresponds to the relative reduction between the overheating escalation factor with and without (reference) system.

$$1 - \frac{\alpha_{sys}}{\alpha_{ref}} \quad (16)$$

The *daily maximum perceived cooling* is calculated by comparing the difference between the 25,6°C limit temperature and the maximum average daily $SET^*_{dailymax}$ value obtained with the system to that obtained without the system (reference) (17).

$$1 - \frac{SET^*_{dailymax,sys} - 25{,}6}{SET^*_{dailymax,ref} - 25{,}6} \quad (17)$$

The relative dimensionless values provide a coherent comparison of all the indicators on a radar chart (Figure 12), making it easier to analyze performance according to the simulated climates.

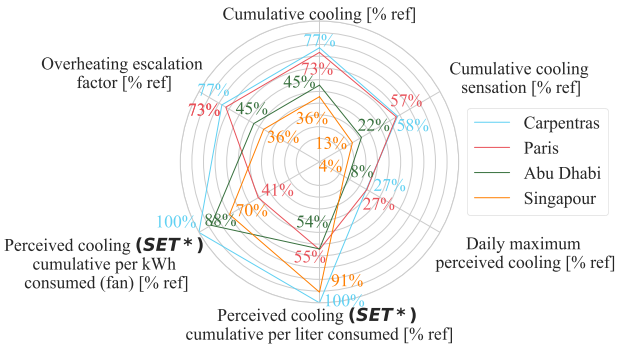

Figure 12: Relative values of system performance for four climates

This graph illustrates the relative performance of the system in four different climates. The further a curve is from the center, the better the performance.

The trends observed confirm the results of the absolute values presented in Table 1. The Carpentras climate is the most suitable for this type of system. In fact, the graph shows that the area corresponding to the Carpentras curve is twice that of Paris and 2,6 times that of Abu Dhabi. On the other hand, humid climates such as Singapore do not provide ideal outdoor conditions for efficient operation, except when the reduction of overheating by the volume of water evaporated is taken into account. Warm, dry climates are more suitable for the system as they better limit indoor overheating while optimizing the water and fan energy consumption.

4. Conclusions

The aim of this study was to evaluate the performance of adiabatic cooling with free cooling and AHU for tertiary buildings. Overall, the results show that the system performs best in the Mediterranean climate, offering the best balance between water and energy consumption, as well as its potential to reduce overheating. In arid climates, outdoor conditions increase the potential for adiabatic cooling, reducing the need for free cooling and full fan

https://doi.org/10.26868/25222708.2025.1364

power, which in turn reduces the energy consumption of fan. On the other hand, in equatorial climates, high humidity limits water evaporation, reducing the cooling potential of the adiabatic system, which in turn limits system performance. On the other hand, increased use of free cooling can better mitigate overheating while minimizing water consumption, but may affect overall efficiency due to fan energy consumption.

Thus, while hot, dry climates offer the best performance, equatorial and continental climates each offer specific advantages depending on the indicators selected. These results highlight the importance of adapting system management to climatic conditions. Although specific to a given configuration, system parameters can be adjusted to optimize performance in any climate.

Acknowledgement

This study is financially supported by the National Association of Research and Technology (ANRT, France) (No. 2022/1087).

References

ASHRAE, 2013. ANSI/ASHRAE Standard 55-2013.

Attia, S., Holzer, P., Homaei, S., Kazanci, O.B., Zhang, C., Heiselberg, P., 2022. Resilient Cooling in Buildings – A Review of definitions and evaluation methodologies. CLIMA 2022 conference. https://doi.org/10.34641/clima.2022.195

De Angelis, A., Saro, O., Truant, M., 2017. Evaporative cooling systems to improve internal comfort in industrial buildings. Energy Procedia, ATI 2017 - 72nd Conference of the Italian Thermal Machines Engineering Association 126, 313–320. https://doi.org/10.1016/j.egypro.2017.08.245

Gagge, A., Fobelets, A., Berglund, L., 1986. A standard predictive index of human response to the thermal environment. Ashrae Transactions 92, 709–731.

Hamdy, M., Carlucci, S., Hoes, P.-J., Hensen, J.L.M., 2017. The impact of climate change on the overheating risk in dwellings—A Dutch case study. Building and Environment 122, 307–323. https://doi.org/10.1016/j.buildenv.2017.06.031

IPCC, 2022. AR6 Climate Change 2022: Mitigation of Climate Change — IPCC. URL https://www.ipcc.ch/report/sixth-assessment-report-working-group-3/ (accessed 12.12.22).

Jia, L., Liu, J., Wang, C., Cao, X., Zhang, Z., 2019. Study of the thermal performance of a novel dew point evaporative cooler. Applied Thermal Engineering 160, 114069. https://doi.org/10.1016/j.applthermaleng.2019.114069

Kashyap, S., Sarkar, J., Kumar, A., 2020. Exergy, economic, environmental and sustainability analyses of possible regenerative evaporative cooling device topologies. Building and Environment 180, 107033. https://doi.org/10.1016/j.buildenv.2020.107033

Kowalski, P., Kwiecień, D., 2020. Evaluation of simple evaporative cooling systems in an industrial building in Poland. Journal of Building Engineering 32, 101555. https://doi.org/10.1016/j.jobe.2020.101555

Machard, A., Inard, C., Alessandrini, J.-M., Pelé, C., Ribéron, J., 2020. A methodology for assembling future weather files including heatwaves for building thermal simulations from the european coordinated regional downscaling experiment (Euro-Cordex) climate data. Energies 13, 3424. https://doi.org/10.3390/en13133424

Maisotsenko, V., Gillan, L.E., Heaton, T.L., Gillan, A.D., 2003. Method and plate apparatus for dew point evaporative cooler. US6581402B2.

Mohammed, R.H., El-Morsi, M., Abdelaziz, O., 2022. Indirect evaporative cooling for buildings: A comprehensive patents review. Journal of Building Engineering 50, 104158. https://doi.org/10.1016/j.jobe.2022.104158

PROFEEL, 2021. Les solutions de rafraichissement adiabatique dans les bâtiments tertiaires en rénovation. Profeel. URL https://programmeprofeel.fr/ressources/guide-les-solutions-de-rafraichissement-adiabatique-dans-les-batiments-tertiaires-en-renovation/ (accessed 6.20.23).

Watt, J.R., 1997. Evaporative air conditioning handbook, 3rd ed. ed. Fairmont Press, Lilburn, GA, Upper Saddle River, NJ.

WMO, 2024. OMM [WWW Document]. WMO. URL https://wmo.int/news/media-centre/2024-track-be-hottest-year-record-warming-temporarily-hits-15degc (accessed 12.16.24).

Xuan, Y., Xiao, F., Niu, X., Huang, X., Wang, S., 2012. Research and application of evaporative cooling in China: A review (I)–Research. Renewable and sustainable energy reviews 16, 3535–3546.